

33B.0 IN-SITU STUDIES OF STRAIN RATE EFFECTS ON PHASE TRANSFORMATIONS AND MICROSTRUCTURAL EVOLUTION IN MULTI-PRINCIPAL ELEMENT ALLOYS

John Copley (Mines)

Faculty: Amy Clarke (Mines)

Other Participants: Francisco Coury (UFSCar)

Industrial Mentor: Clarissa Yablinsky (LANL), Paul Wilson (Boeing), John Foltz (ATI)

This project initiated in Fall 2018 and is supported by the Office of Naval Research. The research performed during this project will serve as the basis for a MS thesis program for John Copley.

33B.1 Project Overview and Industrial Relevance

Multiple Principle Element Alloys (MPEAs) have gained recent interest, as they represent a relatively unexplored alloy design space, being centered in, rather than at, the corners of ternary, quaternary and quinary phase diagrams [33B.1]. Some MPEAs, especially those from the CoCrNi family, have the potential to exhibit transformation and twinning induced plasticity (TRIP and TWIP respectively), where plastic deformation is accommodated by shifts in the stacking sequence of specific atomic planes, in addition to dislocation motion [33B.2]. The combination of TRIP/TWIP, in addition to dislocation motion and multiplication, results in high work hardening rates, as the boundaries of transformation product and twin interfaces act as barriers to dislocation motion [33B.3]. Materials with high work hardening rates are, in turn, associated with increased ductility and strength when compared to materials with otherwise similar properties and lower work hardening rates, as predicted by the Considère instability criterion $\sigma = d\sigma/de$. The influence of strain hardening rate on ultimate tensile strength and uniform elongation in a tensile test is illustrated in **Figure 33B.1**. Increasing the ductility of a material without a corresponding decrease in strength increases the area under the stress-strain curve. A larger area under a stress strain curve indicates a larger specific plastic work to fracture, which is one measure of toughness.

Materials with high toughness are useful in engineering applications, as they are able to absorb higher amounts of energy before failure. High energy absorption is especially useful for blast resistance, which is the primary focus of this project. Increased energy absorption/toughness reduces the required amount of armor for similar protection against explosive reactions. Outside of blast resistance, the extended ductility of TRIP/TWIP materials improves their formability, allowing them to be worked into complex geometries that require higher strains. Studies of the effects of strain rate and state, as well as phase stability and deformation mechanisms, on the deformation behavior and microstructural evolution of MPEAs will enable alloy design for specific applications. Furthermore, better fundamental understanding of TRIP/TWIP behavior extend to more commonly used high strength steels that exhibit TRIP/TWIP behavior, in addition to metastable β -titanium alloys – a complementary project underway in CANFSA.

33B.2 Previous Work

33B.3.1 Literature Review

A review of the existing literature reveals a few families of MPEAs that have received much attention. The Cantor Alloy, an equi-atomic CoCrFeMnNi FCC solid solution, has been shown to be the toughest true high-entropy-alloy (with an entropy of mixing greater than 1.5R) [33B.1]. Work by George *et al.* has shown that the equiatomic CoCrNi medium entropy alloy has superior strength and ductility relative to the Cantor alloy [33B.4]. Work on CoCrNi equi-atomic alloys has shown the formation of nano-twins during deformation resulting in enhanced strength and toughness at cryogenic temperatures when twinning becomes more prominent [33B.5]. Relative to other material systems, CoCrNi alloys have promising combinations of strength and ductility. Accordingly, the CoCrNi ternary system was selected as a system of interest in this work. Work performed by Coury *et al.* using a solid solution strengthening model designed for HEAs, called effective atomic radii for strength (EARS), suggested superior properties are available for non-equiatomic compositions [33B.6]

33B.3.2 Initial Investigation of TRIP in Co₅₅Cr₄₀Ni₅

Evidence of TRIP behavior in a Co₅₅Cr₄₀Ni₅ MPEA was seen following cold rolling to 25% by Dr. Francisco Coury during his PhD work. Initial microstructural characterization of the cold rolled material showed the presence of both

deformation twins and transformation product. Thermo-Calc modeling of T_0 , the temperature at which two phases have the same free energy and the same composition, indicated a high T_0 (above 900°C) for this alloy. A high T_0 temperature indicates that a diffusionless transformation (and the possibility of TRIP) can occur at elevated temperatures. A 2 kg ingot of the $\text{Co}_{55}\text{Cr}_{40}\text{Ni}_5$ alloy was prepared via spray-forming at the Federal University of Sao Carlos (UFSCar), in Brazil by Dr. Guilherme Zepon. This ingot was used in in-situ synchrotron x-ray diffraction (XRD)/thermo-mechanical experiments conducted by Dr. Francisco Coury at the Brazilian Light Source (LNLS). The XRD/thermo-mechanical tests were conducted using quasi-static strain rates at a variety of temperatures, ranging from -100°C to 900°C. The XRD data show transformation of the FCC phase to HCP during deformation in all tests conducted from -100°C to 450°C. Data showing the appearance of an HCP phase in the XRD data with increasing strain is included as **Figure 33B.2**. For temperatures above 450°C, the XRD data does not show evidence of the HCP phase, indicating the deformation-induced transformation is suppressed. The stress-strain data from tensile tests conducted at temperatures between -100 °C and 750 °C are shown in **Figure 33B.3**. Premature failure may have occurred in these samples, due to defects/pores that formed during the spray forming process. Spray forming was initially used to allow for larger scale production of MPEAs compared to arc melting. There is a difference in the work hardening response to strain between the low temperature tests where transformation occurs and the high temperature tests where XRD data suggests no transformation occurs. These changes in mechanical behavior, combined with XRD data, suggest a difference in deformation mechanism consistent with high temperature suppression of TRIP behavior.

33B.3.3 High Rate Experiments at the APS in Early 2019

This project, as well as its compliment focusing on metastable β -titanium alloys (Project #33A), were awarded beam time from a general user proposal at the Advanced Photon Source (APS) at Argonne National Laboratory. In-situ XRD and Kolsky bar (Split-Hopkinson bar) compression and tension experiments were conducted at the APS 32-ID-B beamline, with the goal of observing x-ray diffraction evolution due to TRIP behavior at high strain rates (on the order of 10^3 s^{-1}) and dynamic response during deformation. Four alloys were selected using Thermo-Calc modelling of the diffusionless transformation temperature ($\text{Co}_X\text{Cr}_{40}\text{Ni}_{60-X}$ where $X=55, 50, 40,$ and 30 at.%, hereafter referred to by their Cobalt content) and the equi-atomic CoCrNi, were produced by arc melting. These alloys were selected to have a wide range of T_0 and be within the single phase FCC region at 1100°C. Analysis of the XRD data shows the evolution of a few individual spots to diffuse rings upon deformation, indicating crystallite refinement possibly from the formation of deformation twins, as illustrated in **Figure 33B.4**. Use of HiSPoD, or High Speed Polychromatic Diffraction, a matlab program built to analyze data collected during high speed in-situ experiments at Sector 32 at the APS allowed for rapid processing of the collected in-situ XRD data [33B.7]. In the CoCrNi samples, high absorbance by the material resulted in relatively low diffracted intensities and complications due to the polychromatic nature of the “pink” beam at the APS. Efforts to solve this in anticipation of future beam time allocations are discussed in Section 33B.3.1

33B.3 Recent Progress

33B.3.1 Sample Thickness Effects on Diffraction Results at the APS

During the in-situ XRD and dynamic straining experiments performed at the APS in Feb 2019, several sample size related issues evolved. The Kolsky Bar device at Sector 32 is energy limited, and some tensile specimens failed to fracture during the initial loading. In Kolsky Bar tension experiments, if a sample fails to break, it becomes cyclically loaded, and microstructural changes that evolve from the high strain rate deformation become convoluted with effects of the cyclic loading. Additionally, the polychromatic beam (“pink” beam has two peaks, the first and more intense at 24keV, and the second at 46keV). Dual sets of rings for every peak are anticipated when correcting for the material’s absorption. The relative intensity and spacing of the rings from the low energy and high energy peaks make in-situ observations of phase transformations difficult for these materials. A simulation of the diffraction for this material, using a 500 μm thick sample, is shown in **Figure 33B.5**. The high intensity, low angle peaks are associated with the 2nd harmonic which has its peak at approximately 46keV, while the lower intensity peaks are associated with the 1st harmonic which peaks at about 24keV. Nominally, the 1st harmonic is much more intense, but is more easily absorbed by materials like CoCrNi due to its lower energy. The result is difficulty in discerning changes in peak intensity during the test. An investigation into the requisite sample thickness to eliminate this issue was undertaken using the diffraction simulation portion of the HiSPoD program. Selected results are also included in **Figure 33B.5**. Essentially, thinner

samples alleviate this problem, as well as the issues with fracture during the initial straining cycle, but become more difficult to produce and less representative of bulk behavior. Both 100 μ m and 250 μ m samples will be prepared for additional time at the APS.

33B.3.2 Material Preparation and Heat Treatment for Upcoming Testing

In anticipation of additional time at the APS, as well as a need to perform mechanical testing at the lower strain rates achievable at Mines, methods of sample preparation are being tested. Some material has been produced by Dr. Coury at UFSCar, specifically the Co-40 and Co-55 alloys, in bulk, allowing for sub-sized tensile specimens to be cut directly from the cast block. Other alloys are being produced by arc melting from high purity components. These buttons mass approximately 50g and are not geometrically suited for machining. Further, initial attempts at melting resulted in buttons with inhomogenities associated with incompletely melted starter material. Additional flipping and increased amperage used have eliminated these inhomogenities in the most recently prepared buttons. The buttons can be rolled to nearly 80% reduction in height without cracking, allowing them to be rolled to better geometries for sample machining. It was anticipated that sample machining could begin recently, however, heat treatment to a single phase of these alloys remains difficult. Literature suggests, for an equiatomic CoCrNi alloy, a post cold rolling annealing at 1100-1200°C [33B.4,5] but XRD taken on deformed and annealed samples with similar compositions after 2 hours at 1150°C show peaks associated with the HCP phase. One such XRD scan is shown as **Figure 33B.6**. The selected material for the scan, Co-30 is not predicted to experience a martensitic FCC-HCP transformation, so any HCP fraction should be remnant from HCP formed during the annealing process.

33B.4 Plans for Next Reporting Period

Material is available for mechanical testing to take place in the near term. Plans for the next reporting period include:

- Investigation of proper heat treatments for FCC solid solutions post cold rolling and annealing.
- Conduct tensile testing at various strain rates achievable at Mines on the range of selected CoCrNi alloys.
- Prepare samples for, and perform future experiments at the APS and at the Cornell High Energy Synchrotron Source (early 2020).
- Post-mortem analysis of microstructural changes during deformation by means of XRD and EBSD of alloys strained at low and high rates.

33B.5 References

- [33B.1] D.B. Miracle, J.D. Miller, O.N. Senkov, C. Woodward, M.D. Uchic, J. Tiley, Exploration and Development of High Entropy Alloys for Structural Applications, *Entropy* 16 (2014) 494-525.
- [33B.2] Y. Deng, C.C. Tasan, K.G. Pradeep, H. Springer, A. Kostka, D. Raabe, Design of a twinning induced plasticity high entropy alloy, *Acta Materialia* 94 (2015) 124-133.
- [33B.3] L. Liu, B. He, M. Huang, The Role of Transformation-Induced Plasticity in the Development of Advanced High Strength Steels, *Advanced Engineering Materials* article number 1701083 (2018).
- [33B.4] G. Laplanche, A. Kosta, C. Reinhart, J. Hunfeld, G. Eggeler, E.P. George, Reasons for the superior mechanical properties of medium-entropy CrCoNi compared to high-entropy CrMnFeCoNi, *Acta Materialia* 128 (2017) 292-303.
- [33B.5] B. Gludovatz, A. Hohenwarter, K. Thurston, H. Bei, Z. Wu, E.P. George, R. Ritchie, Exceptional damage-tolerance of a medium-entropy alloy CrCoNi at cryogenic temperatures, *Nature Communications* article number 10602 (2016).
- [33B.6] F. Coury, K. Clarke, C. Kiminami, M. Kaufman, A. Clarke, High throughput discovery and design of strong multicomponent metallic solid solutions, *Scientific Reports*. 8 (2018) Article number 8600.
- [33B.7] T. Sun, K. Fezzaa, HiSPoD: a program for high speed polychromatic X-ray diffraction experiments and data analysis on polycrystalline samples, *Journal of Synchrotron Radiation*, Vol. 23(4) (2016) 1046-1053.

33B.6 Figures and Tables

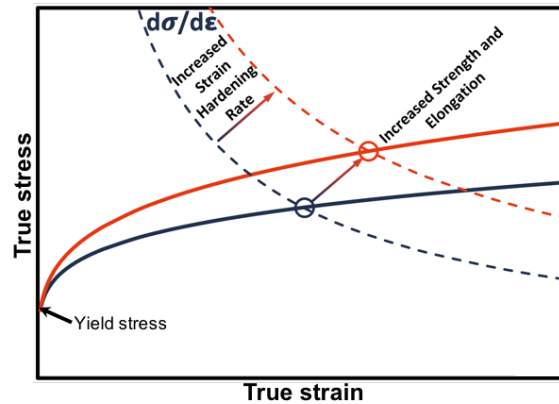


Figure 33B.1: Schematic stress strain curves for two materials with similar properties (elastic modulus, yield strength), but with different work hardening rates. Predicting the onset of necking by the instability criterion, $\sigma = d\sigma/d\epsilon$, shows an increase in both ultimate tensile strength and uniform elongation associated with an increase in work hardening rate.

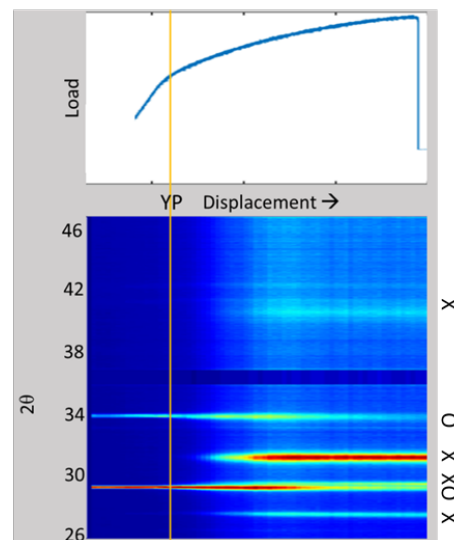


Figure 33B.2: XRD and load-displacement data for the $\text{Co}_{0.55}\text{Cr}_{0.40}\text{Ni}_{0.05}$ alloy tested at 60°C , showing the evolution of HCP phase at the expense of the FCC. The transformation begins almost immediately post yield (the temporal resolution of the XRD is insufficient to determine if some small strains exist before transformation). Testing performed by Dr. Francisco Coury at the Brazilian Synchrotron Light Laboratory (LNLS) using x-rays with wavelength of 1.033\AA . Peaks associated with the HCP phase are marked with an X and those associated with the FCC phase are marked with an O.

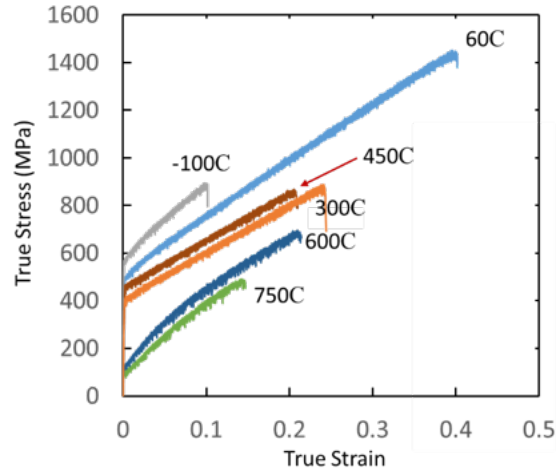


Figure 33B.3: True stress-true strain curves for the $\text{Co}_{0.55}\text{Cr}_{0.40}\text{Ni}_{0.05}$ alloy for multiple test temperatures. Porosity from the spray forming process may have led to premature failure of the samples, as indicated by an arrow in the 450 °C test.

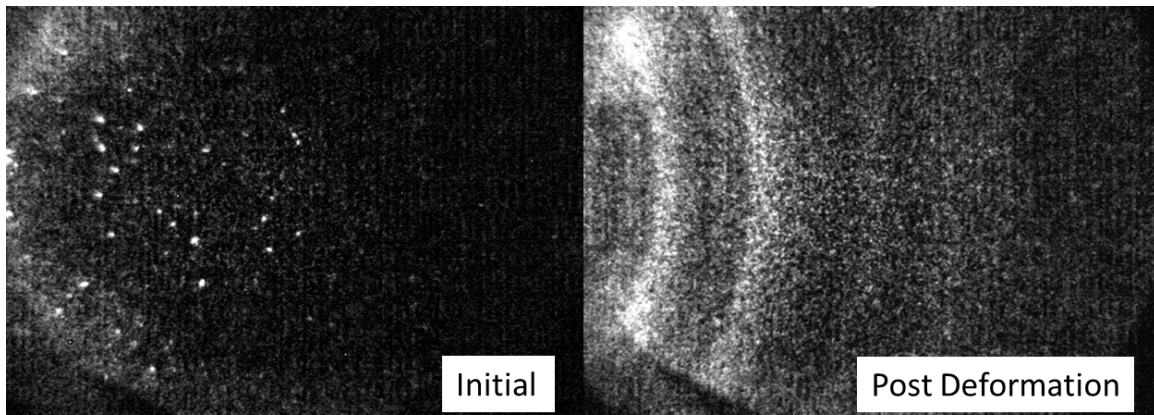


Figure 33B.4: Diffraction patterns collected for a Co-40 compression cylinder before and after deformation, showing the evolution of full diffraction rings from originally spotty patterns. This is indicative of domain refinement, and in alloys known to experience significant deformation twinning, is suggestive of TWIP behavior.

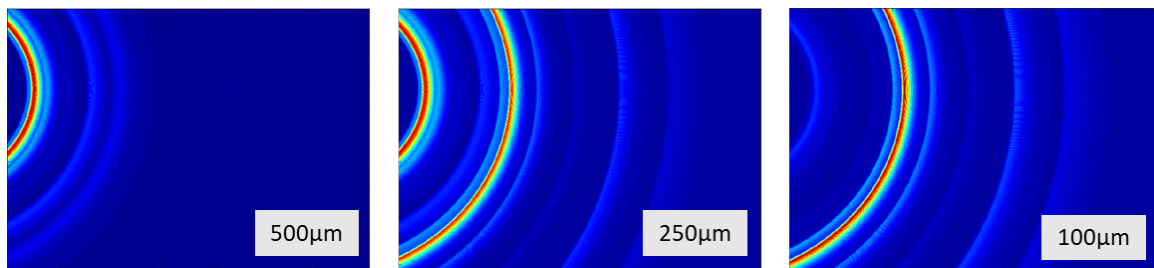


Figure 33B.5: Simulated diffraction patterns showing absorption corrected diffraction intensities of a Co-50 alloy for various achievable thicknesses. Thinner samples reduce the relative intensity of the 2nd Harmonic (the rings closest to the upper left) but are less representative of bulk properties.

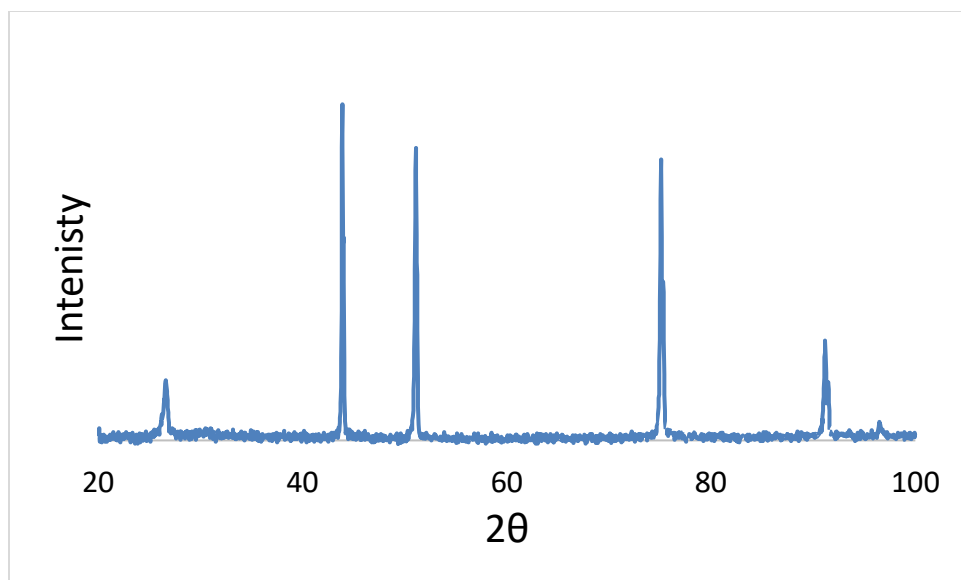


Figure 33B.6: XRD pattern collected from a Co-30 sample that had been cold rolled to 75% reduction in height and annealed at 1150°C for 2 hours. The pattern shows a peak at 26.6° which cannot be attributed to any FCC allowed reflections.